Genetic Algorithm Based Approach of SRM Current Profiling for Torque Control and Minimal Copper Losses

Euan MacRae
Department of Electronic and Electrical Engineering
University of Strathclyde
Glasgow, Scotland, UK
euan.macrae@strath.ac.uk

Ali Abdel-Aziz
Department of Electronic and Electrical Engineering
University of Strathclyde
Glasgow, Scotland, UK
ali.hassan-abdelaziz-ali@strath.ac.uk

Khaled Ahmed
Department of Electronic and Electrical Engineering
University of Strathclyde
Glasgow, Scotland, UK
khaled.ahmed@strath.ac.uk

Richard Pollock
Technelec.ltd
Oakham, England, UK
richard.pollock@tehnelec.co.uk

Barry W Williams
Department of Electronic and Electrical Engineering
University of Strathclyde
Glasgow, UK
barry.williams@strath.ac.uk

***Abstract*— This paper presents a novel approach to current profiling for switched reluctance machines that eliminates torque ripple while inherently guaranteeing minimum copper losses, along with linear torque control. Minimization of copper losses increases machine efficiency, while eliminating torque ripple is the pre requisite for SRM use in applications such as traction vehicles. This paper presents theoretical optimal current profiles, initially without consideration of DC link voltage limitations. Utilizing a Genetic Algorithm in conjunction with current profiling limit envelopes, an optimized set of current profiles across the torque ripple free speed range of an exemplary 8/6 SRM is then created. The profiles characteristics are analyzed and compared with commonly used torque sharing function control to confirm the merits of the proposed method.**

Keywords — Current Profiling, Electric Vehicles, Genetic Algorithm, Switched Reluctance Machine

I. Introduction

The switched reluctance machine (SRM) has recently received renewed interest, due to its characteristics that make it potentially an attractive alternative in applications such as electric vehicles (EVs) [1]-[2]. From an environmental and cost perspective, possibly the main advantage of the SRM is its lack of costly permanent magnet material in its robust rotor construction. It also offers good fault tolerance owing to its relatively simple design which is desirable [3], but suffers from a relatively low power factor (recovered inductive energy), problematic acoustic noise due to undesirable tangential torque ripple whence radial stator deforming forces, and nonlinear magnetic characteristics. This makes the machine difficult to control [4]. For the machine to be an alternative to machine designs used in EVs such as the permanent magnet synchronous machine (PMSM) or induction machine (IM), its efficiency must be optimized, torque ripple eliminated, and torque control linearized.

Inherent in the SRMs doubly salient design, the resultant discrete torque production and nonlinear nature of the machine can result in torque ripple. If no specific strategy is taken to prevent this, significant net torque ripple (TR) typically occurs at phase commutation such as when using basic square wave control.

Many SRM control strategies exist that reduce or eliminate torque ripple. Comparably to the numerous proposed machine design alterations [5]-[8], control methods offer superior cost efficiency and ease of implementation, with minimal changes required to the SRMs structure [6].

For examples of direct control strategies, direct torque control (DTC), and a popular development from DTC, direct instantaneous torque control (DITC) have been presented in literature. DTC is first proposed in [7], where torque is estimated using a *(T-I-θ)* Lookup Table (LUT), a derived rate of change of a stator flux vector then indicates the flux and conduction period, which is regulated by a hysteresis band controller. This results in online torque ripple reduction but requires accurate machine parameters and a variable switching frequency. In many ways similar to DTC, rather than accurate position sensing and flux control, the DITC method in [8] proposes instantaneous estimation of machine torque solely from the terminal values of phase currents and voltages. Estimation is carried out using a *(T-I-λ)* LUT, where flux linkage, λ, is calculated using the terminal voltage with consideration to stator winding losses. Its advantages are similar to DTC but also has the added benefit of not requiring a high-resolution position encoder and is adaptable for further optimization such as for EVs [9] or a general scheme [10].

Indirect torque control schemes can also be employed; one online approach being optimization of the phase turn-on and turn-off angles. In [11], the turn-on angle is determined by any change in machine speed or phase rms current. The turn-off angle is then calculated to introduce the optimal flux linkage decay during phase commutation with overlap between the outgoing phase and incoming phase turn-on. This mitigates torque ripple at commutation but allows little adjustability if any manipulation of the current profile or torque is desired. An online or offline approach known as current profiling is also applicable to SRMs and can take many forms. The general approach involves the construction of phase current profiles for the machine based upon some optimization criteria. In the offline case, as in this paper, these profiles are pre constructed and stored in a LUT. In the online case, profiles are calculated in real time where both methods then feed the data for conversion to drive control signals. An example of this is [12], where optimal profiles are constructed using stored single-phase current profiles for various linearized torque levels across the conduction range of a 4φ SRM. It introduces torque sharing between phases without the use of an online function before torque sharing functions (TSFs) were established in the literature. TSFs are a popular strategy employed in SRM control for eliminating the machines inherent torque ripple, having been implemented in many forms [13]. They operate from the principle of *torque sharing* at current commutation where the outgoing phase and

This is a peer-reviewed, accepted author manuscript of the following conference paper: MacRae, E, Abdel-Aziz, A, Ahmed, K, Pollock, R & Williams, BW 2023, Genetic algorithm based approach of SRM current profiling for torque control and minimal copper losses. in 2023 IEEE International Electric Machines & Drives Conference (IEMDC). IEEE, Piscataway, NJ. https://doi.org/10.1109/IEMDC55163.2023.10239015

the sequential phase conduct simultaneously. This introduces an overlap between phases based upon some designed mathematical function that distributes torque between phases that achieves up to FLT production with theoretically no ripple.

In the literature, various optimization techniques have been applied to better existing control schemes. Novel SRM approaches are becoming less common. Algorithmically, TSFs have been improved online using methods such as an Ant Colony algorithm in [14] that optimizes switching angles, extending the speed range of the machine while minimizing rms current or [15] where the same is accomplished using a computationally expensive exhaustive search algorithm. DTC is optimized in [16], using recently developed wolf and coyote meta-heuristic approaches to reduce torque ripple and stabilize speed control as a substitute to traditional PI control of a DTC scheme.

This paper presents a novel method of SRM current profiling with a new Generic Algorithm (GA) design which utilizes phase torque sharing and a delayed turn-on angle. The first criteria needed for the algorithm is a minimal rms current that is a theoretical parameter obtained by allowing infinite DC link voltage. The algorithm then uses this seed as a target to produce an optimized profile at a given speed and this process is repeated across the SRMs ripple free speed range.

TABLE I
SPECIFICATIONS OF SRM (4KW AT 1500RPM)

Parameter	Value	Parameter	Value
No. of motor phases m	4	Rotor outer radius	45mm
Stator/rotor poles N_s/N_r	8/6	Thickness of rotor yoke	15mm
stator pole arc/ pole pitch	0.42	Motor axial length	155mm
rotor pole arc/pole pitch	0.35	Stator inner radius	46mm
Turns per pole N	90	Stator outer radius	83mm
DC link voltage V_{dc}	415V	Thickness of stator yoke	12mm
Phase resistance R	0.8Ω	Shaft radius	15mm

The structure of the paper is as follows: Section II introduces a novel approach for calculating the theoretically absolute minimal rms current profile for any SRM configuration that is 3-phases or more. Section III introduces the GA design to accomplish what is established in Section II with DC link voltage limitation considered. Finally, Section IV validates the GA design using simulation results that compare operation of the GA produced profiles in a LUT versus current profiles produced using a Cosine TSF. Table 1 provides the characteristics of the exemplary 8/6 SRM used in this paper.

II. PROPOSED THEORETICALLY MINIMAL RMS CURRENT TORQUE CONTROL METHOD

At low speeds, DC link voltage is not a limiting constraint. By implementing phase commutation torque sharing, current profiling can be used to establish the idea of a profile with the theoretically lowest rms current for zero torque ripple (ZTR). The proposed method establishes a conduction period for the positive torque region from 30° to 60°, where successive phases are enabled to overlap by the maximum overlap angle θ_{ov} to maintain 2-phase torque sharing in TSFs (1) using the rotor pole pitch θ_r and stroke angle ε (2).

$$\theta_{ov} \leq \tfrac{1}{2}\theta_r - \varepsilon = \tfrac{1}{2} \times 60^\circ - 15^\circ = 15^\circ \quad (1)$$

$$\varepsilon = \frac{2\pi}{mN_r} = \frac{2\pi}{4 \times 6} = 15^\circ \quad (2)$$

At each angular step, combinations of torque that fulfil full load torque (FLT) demand are created. Each phase has a range from 0-25Nm in this case, and are given the option to either overlap (where both phases produce torque) or allow a single phase to produce FLT. To obtain the current values for torque combinations that satisfy the FLT demand and also consider DC link voltage, a relationship must be established between torque T, current I, flux linkage λ and the rotor angle θ. This is accomplished using Ansys Maxwell finite element analysis of the 8/6 machine in question, producing two LUTs that relate $T - i - \theta$ and $\lambda - i - \theta$ respectively. Pairings of currents can then be created that represent these torque combinations. Using these parings, at each angular step a comparison can be made to gauge the optimal currents for use in the profile. This is based upon a loss variable K_{Cu} (3) that is indicative of the magnitude of total copper losses.

$$K_{Cu} = {I_A}^2 + {I_B}^2 \quad (3)$$

Table II is an example of these calculations at 39.5° and the respective angle 54.5° where phases can overlap. Each axis shows the torques and respective currents that each phase

TABLE II
CURRENT PAIRING SELECTIONS AT 39.5° AND 54.5° FOR FOUR TORQUE LEVELS

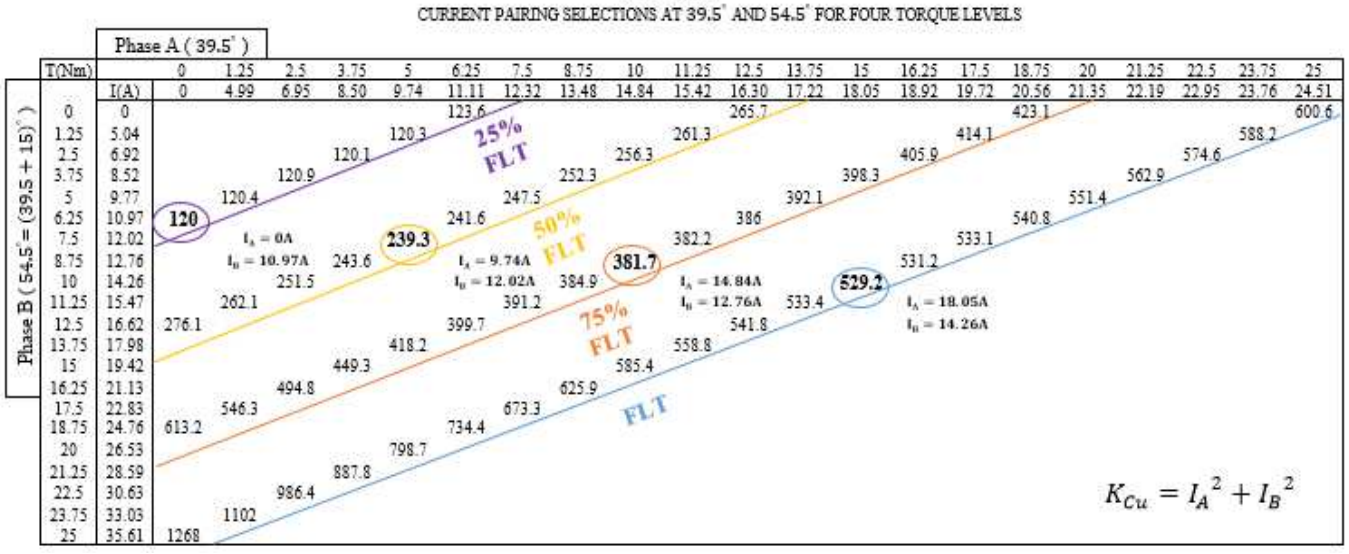

can produce. In the main grid, each line represents four torque level from 25-100% of FLT. They underscore the K_{Cu} values of the currents needed to fulfil said torque demands at each level. Highlighted on each diagonal are the optimally minimal K_{Cu} (Cu loss) values for each torque level. Generally, the calculated K_{Cu} values form a valley like shape that flattens as torque demand decreases. The optimal K_{Cu} values follow a decrease in current in Phase A relative to Phase B until Phase B becomes dominant in terms of torque production. For these two angles [39.5° and 54.5° =39.5°+15°], torque is shared near equally between phases until 25% FLT where a single phase is sufficient.

Fig. 1 presents the theoretically optimal profiles produced across torque levels using this torque linearization method with the optimal currents calculated at 39.5º and 54.5 º in Table II. Current rms is based on data stored at 0.1º rotor angle steps and 0.1 Nm incremented torque. Considering the FLT current waveform, it has an rms current of 11.129 A, theoretically the lowest achievable rms current for the given SRM characteristics, at FLT demand with ZTR. With no DC link voltage limitation, when calculating the most efficient torque sharing between phases with the stated θ_{ov}, conduction is not required in low Nm/A efficiency regions near the aligned states of the phase (30° and 60°). (Zero current at alignment also reduces undesirable radial forces, where the radial Nm/A is the highest.) Therefore, high efficiency Nm/A regions can conduct in a single phase for FLT with a small overlap utilizing instantaneous current build-up at phase turn-off (56°) and when the overlap between phases ends (41°). This decrease in conduction period is further exemplified when optimal profiles are constructed across torque levels with the optimal current in Table II highlighted. Observe near zero overlap between phases at lower torque demands.

The linearized torque approach can be extended for three (and higher) phase on operation, for higher phase number SRM machines. For example, third phase $T-i-\theta$ characteristics can be introduced in the Z axis, to create a region for K_{Cu} ($=\Sigma I^2$) for a given torque, at each angle.

This profile in Fig.1 has the mathematically lowest rms current but cannot be implemented practically at meaningful speed with the given DC link voltage. For example, for ZTR FLT at 50rpm, a DC link voltage of 400V suffices, but rates of change in flux linkage λ at turn-off, from 55.99° to 56° at a speed of 500rpm require a 2.8kV rail voltage V_{DC}. This is estimated using the formula that dictates the required DC link voltage (4) [2], where I is the phase current and R_{Cu} is phase stator winding resistance (assumed equal for all phases).

$$V_{DC} - IR_{Cu} = \frac{d\lambda}{d\theta}\omega \qquad (4)$$

III. PROPOSED GENETIC ALGORITHM DESIGN FOR SRM CURRENT PROFILING

The *ideal* profiles (Fig. 1) established in section II, become a target rms (seed) current for the given torque and ripple free speed range of the machine.

Generating valid optimal profiles (with an imposed link voltage restriction) that satisfy the criteria established for this can be computationally expensive at a high resolution; if attempting to create every possible current profile and selecting from the results. The problem can be viewed as an

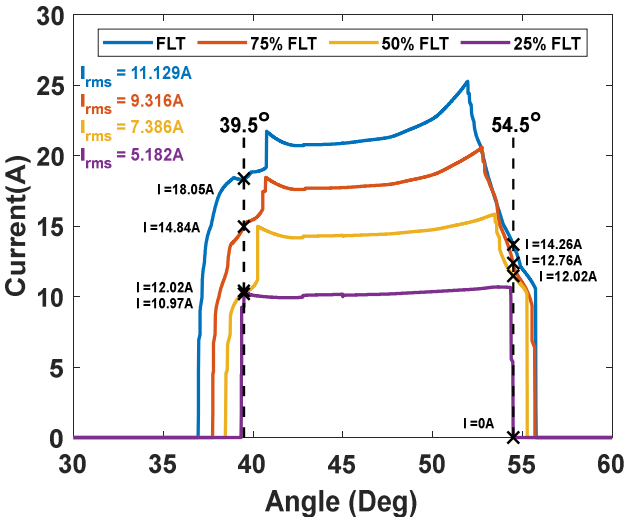

Fig. 1 Theoretically Minimum Current Profiles across FLT levels.

optimization problem that is not easily solved where three conditions are present; namely ZTR, operation at a given speed within V_{DC}, and a minimum rms current. The discrete point by point basis of the current profiles in Fig. 1 are suitable for the format and stages of a GA compared to other optimization techniques in the same meta-heuristic family, such as particle swarm optimization. Apart from this, the technique itself has other notable merits. It produces high quality results to non-linear problems, such as the SRM with its non-linear magnetics and torque production characteristics [17]. It is proposed that current profiling can be carried out using a novel GA design that ensures ZTR, in order to produce optimal current profiles across a wide speed/torque range.

Firstly, the problem is presented as a multi objective problem, with the three prior conditions. This can be simplified for design of an algorithm that is not susceptible to biasing towards specific objectives. In generating a population, at least two objectives are readily solvable; being a valid voltage demand and production of the required torque at every discrete phase pairing in the current profile. Operationally the algorithm maintains these conditions as a prerequisite when altering profiles. It sequentially functions as follows: population generation, crossover, mutation, and evaluation and selection. Each stage bar generation is repeated for either the set amount of iterations or until the optimal rms current is reached.

A. SRM Current Profiling Envelopes

Before randomly generating the algorithm population, the constraints in SRM current profiling for any configuration can be set and visualized which any current profile must be constrained within. Assuming a 2-phase overlap for the given SRM, Fig. 2 illustrates these boundaries at 200rpm with a θ_{on} of 30° and θ_{off} of 60°. FLT is taken as an example.

Examining these limits, firstly an arbitrary limit is set which indicates the rated current of the machine. Secondly to satisfy the requirement of ZTR, either phase must not produce more than FLT at any time unless θ_{on} be delayed, allowing retarding torque to be introduced with $\theta_{off} > 60^{\circ}$. This provides a torque production limit. The remaining limits are

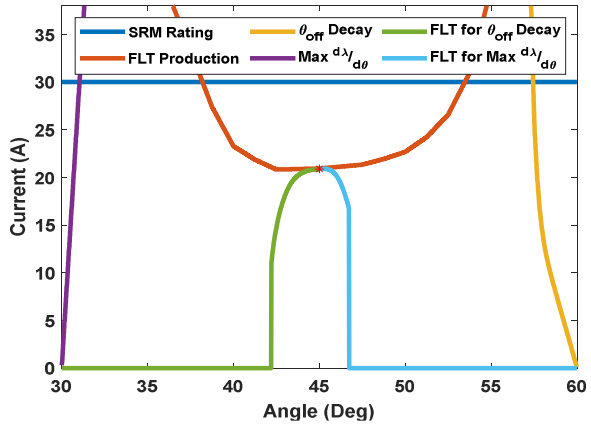

Fig. 2 Current Profiles imposed limits implemented at 200rpm.

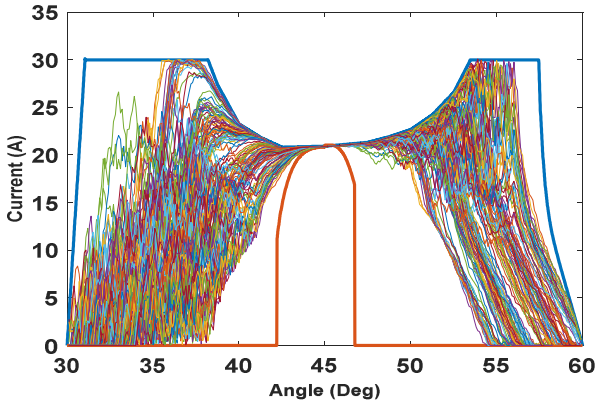

Fig. 3 Initial Generated Population for the GA at 200rpm.

implemented to satisfy speed requirements, where the profile is bounded by its maximum $d\lambda/dt$ from turn on, the reverse limit for FLT production from phase commutation, and the limit which indicates longest conduction path to decay to zero. This limit then imposes a reverse limit on overlapping phase for the profile, again to satisfy FLT production.

With these limits established, various intersect points occur in the conduction period, creating what is in effect an upper and lower envelope as shown in Fig. 3. This dictates the current values that any profile can utilize in its creation to provide FLT and respect the voltage limitations of the drive circuit DC supply. The envelop narrows substantially near the aligned position, where at a θ_{on}= 30˚ and θ_{ov}= 15˚, it is the point where the phases transition from the outgoing to incoming phase in terms of torque sharing. This envelope shifts across speed range and can also be used with an advanced or delayed θ_{on}.

B. Population Generation

To generate a population for the algorithm, the boundary conditions for SRM current profiles are used. Firstly, a grid of current solutions for the incoming phase (30˚ to 45˚) is created from the upper and lower limits of the envelopes and the respective solutions for the outgoing phase (45˚ to 60˚) are created as phase pairings to produce FLT. This can also be done reciprocally with phase *A* as the dominant phase. With the grid of solutions generated, random profiles are generated on a point-by-point basis, with an example shown in Fig. 3 again at 200rpm. Between points while generating, the voltage demand is confirmed for the given speed to be within limits where the next point is only ever selected from

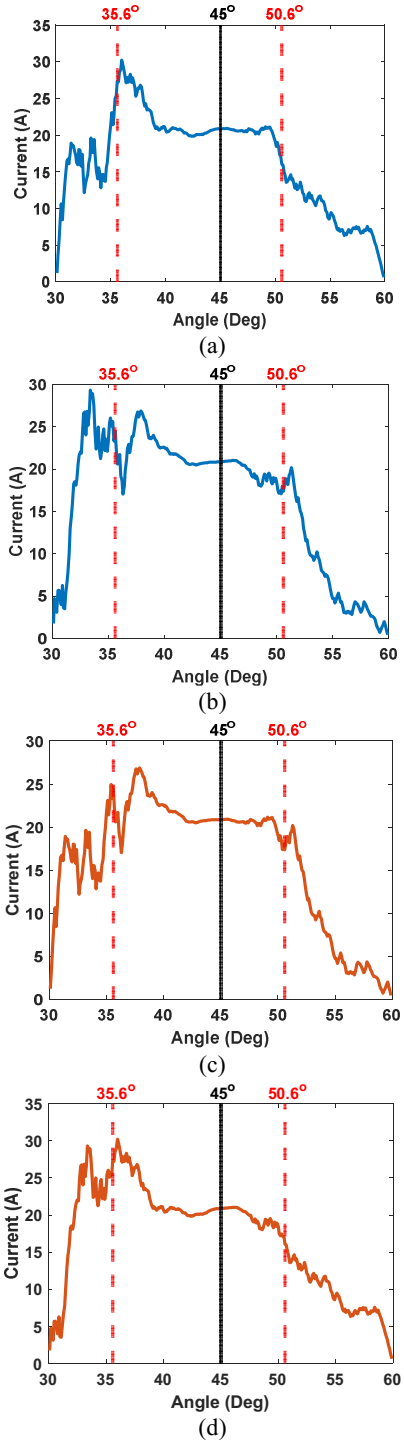

Fig. 4 Crossover Stage carried out at 200rpm for two population members: (a) Parent 1, (b) Parent 2, (c) Offspring 1, and (d) Offspring 2.

solution pairings that are valid for both the incoming and outgoing phases.

C. Profile Crossover

When carrying out crossovers of profiles, torque production does not need to be considered, as any profiles generated as offspring will stem from profiles that already offer ZTR. Fig. 4 conveys this visually, where in order to crossover parent profiles (Fig. 4 parts a and b), a cutting point is randomly chosen, in this case 35.6˚ and 50.6˚. The offspring profiles (Fig. 4 parts c and d) must then be checked

that the new voltage demand at the cutting point is valid for both offspring. If found invalid, a new cutting point is found. The process is then repeated until a possible crossover occurs.

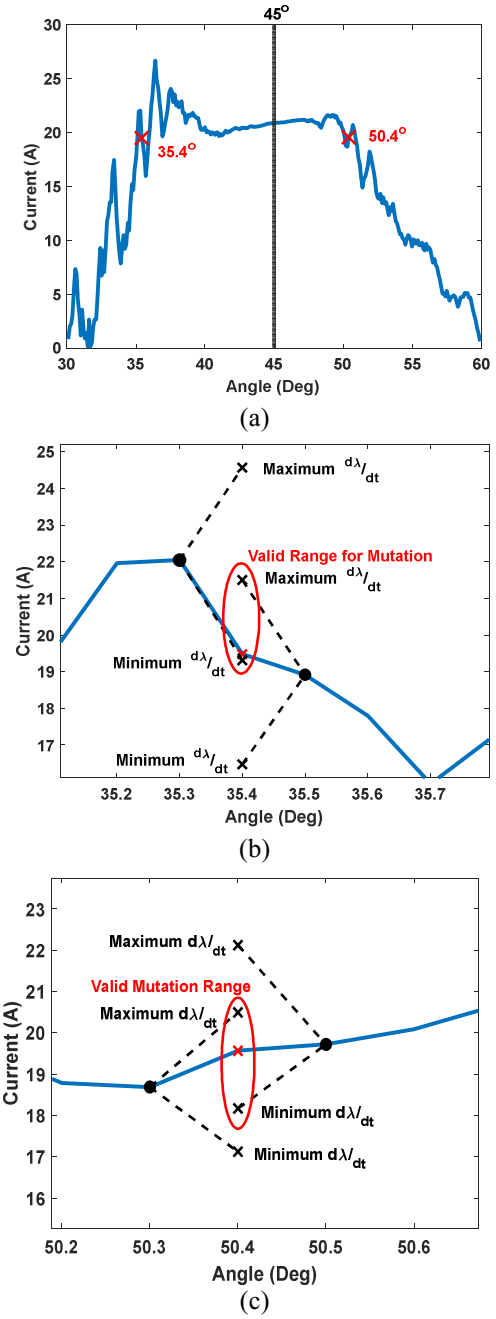

Fig. 5 Mutation Stage carried out at 200rpm: (a) The population member, (b) Incoming Phase Mutation, and (c) Outgoing Phase Mutation.

D. *Profile Mutation*

For profile mutation, checks are made to ensure the profile remains valid for the established conditions. For a given profile, a random mutation point is selected. The first checks that are required relate to the positioning of the mutation. Near turn-on and turn-off of the profiles, any mutation that is carried out must logically not cause two instances of conduction. This for example could be the profile decaying to zero and proceeding to conduct again at a later point in the conduction period. This does not limit mutating a point from zero or to zero. If situated adjacent to a discrete point that is conducting, the algorithm will either increase or decrease the conduction period accordingly within voltage limits. The second check is the range in which the point can be mutated. Fig. 5 conveys this visually, where range of mutation is established by taking the prior and subsequent points in the profile. The maximum $d\lambda/dt$ is then added and subtracted from each point. This confirms the degree of overlap between the four points in Fig.5a. With the overlap determined, a point is randomly selected in the range and the process is repeated for the respective phase in Fig. 5b to create FLT. When this overlap range is created for either phase, a check is made that corrects the minimum or maximum mutation is within envelope boundaries. If a mutation passes these steps, it is deemed valid and replaces the original phase values in the profile. If it is does not, the mutation is discarded, and another point is chosen until a valid mutation is found.

E. *Profile Evaluation and Selection*

As discussed, only one condition is present for the Objective Function to rate being the rms current of the profiles. This can be made as a relatively simple function (5) given that the theoretically absolute lowest rms current is established prior (section II). The function is an absolute measure of proximity to the theoretically optimal rms current with any profile that is measured against it.

$$Fitness = \left(1 - \frac{|I_{RMSOptimal} - I_{RMS}|}{I_{RMSOptimal}}\right) \quad (5)$$

For selection of the profiles that pass to the next generation, a roulette style was chosen. Roulette Wheel selection operates from visualizing the population as a collective fitness value created from summing fitness values of the population representing the *wheel*. The probability of selection is then taken by dividing the individual fitness values by this summation. This creates segments in the roulette wheel where members with larger fitness values have a larger segment based upon the cumulative probability of selection from the population. With these values set, the wheel is spun for how many members that are desired in the new population, with the remainder not chosen, are discarded as the algorithm progresses.

IV. Simulation Results

Fig. 6a presents the results of the designed GA algorithm over the first half of the ripple free speed range for the given FLT and V_{DC} found using SRM current envelopes. The profiles are presented in 100rpm steps from 0 to 500rpm including the theoretically minimum profile introduced in section II, Fig. 1. At the lower end of the speed range at around 100-200rpm the algorithm produces profiles that tend to resemble the theoretical optimal. The profiles begin to lose this shape from 300rpm onwards as the reduced $d\lambda/dt$ begins to extend the decay path of the profiles towards the aligned position. This correspondingly alters θ_{ov} and shape of the profiles in the phase B region, to maintain FLT production, consequently increasing rms current, likely due to the increased conduction period. As profiles approach 500rpm, the θ_{on} of the profiles begins to advance notably as the

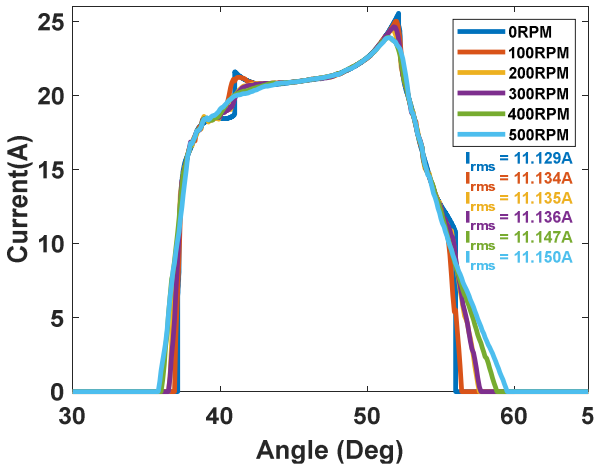

(a)

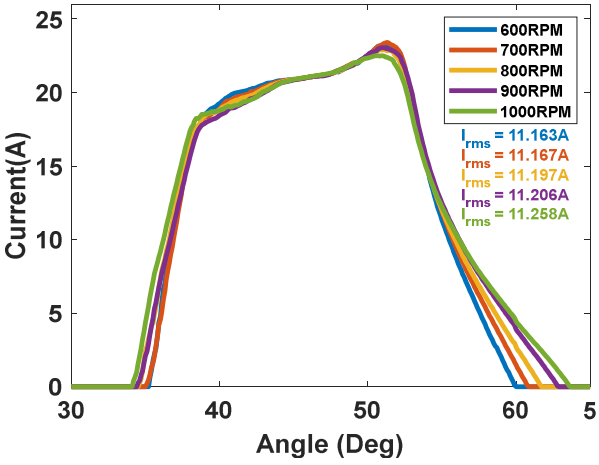

(b)

Fig.6 GA Profiling Results for: (a) 0-500rpm, (b) 500-1000rpm.

optimal build-up to single phase conduction requires a wider conduction period as $d\lambda/dt$ decreases further. This leads to a lower peak current overall but again contributes to a rising rms current as conduction is required in less efficient Nm/A SRM regions of positive torque production angular period.

Fig. 6b shows the algorithm results over the second half of the ZTR speed range given from 600 to 1000rpm in 100rpm increments. In this speed range region, the optimal profiles shapes are dependent on the build-up and decay paths required for the given speed and the combination as such of these and their respective phase pairings that will produce the optimal rms current. In this range, the trend continues of an increasing θ_{ov} coupled with an increasing conduction period. 600rpm represents the profiles reaching the limit of the positive torque production region, where higher speeds introduce retarding torque during their decay paths. Above 800rpm marks a larger disparity in rms current as the profiles advance θ_{on} into more inefficient regions while requiring larger currents and conduction within inefficient negative torque production regions. While the peak current is consistent in still decreasing, it does not contribute to any decrease in rms current as it is required to maintain the FLT and voltage demand conditions of the profiles.

V. Discussion

Fig.7a compares the GA results at 1000rpm and the respective profile using the Cos TSF at FLT with optimal turn

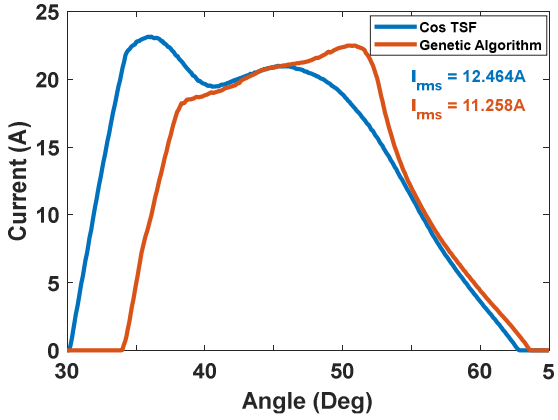

(a)

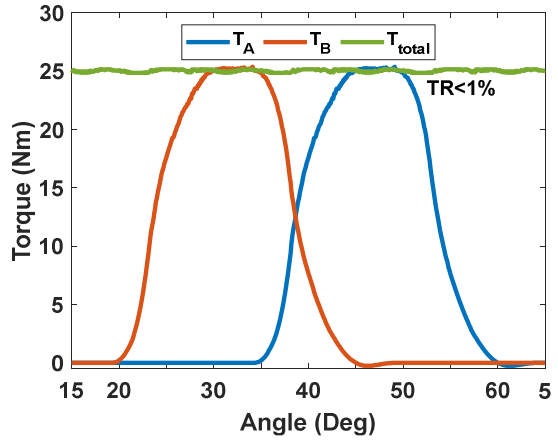

(b)

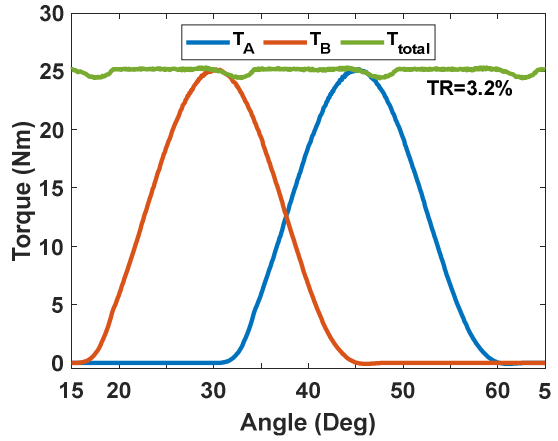

(c)

Fig.7 Comparison between the GA and the Cos TSF at 1000rpm: (a) Current profiles, (b) GA torque waveforms, and (c) Cos TSF torque waveforms.

on/off angles. Note the proposed GA design produces an optimal rms current of 11.258 A (1.16% above the theoretical minimum) compared to 12.464 A for the Cos TSF, at 1000rpm. This merits a 9.7% current decrease (importantly an 18.4% decrease in Cu losses) while still maintaining ZTR operation, shown in Fig.7b. One reason for this decrease is the ability of this design to intentionally utilize retarding torque. At higher speeds, conducting in non-efficient regions near the aligned position at 30° is not optimal as the envelope narrows. This means a delay in θ_{on} is a beneficial trade-off. This is because it allows the profiles to begin conducting for longer in higher Nm/A efficiency regions while introducing a minor amount of inefficient retarding torque (low Nm/A

region). The Cos TSF introduces retarding torque in Fig. 7c but this is unintentional. The profile cannot decay within the given maximum overlap period and leads to three phase conduction seen in Fig. 7a where conduction exceeds $½\theta_r$ .This contributes to torque ripple as the TSF cannot compensate without modification.

In comparison to the theoretically minimum current produced; (Section II, Fig. 1a); the increase across the speed range from 0 to 1000rpm only displays a maximum increase in rms current of 1.16%. As part of a control scheme this can be implemented in a LUT format at the given FLT of 25 Nm from 0 to 1080rpm, being the ZTR limit of the 8/6 SRM two phase conduction with the given V_{DC} of 415V dc. Fig.8 conveys this along with the whole ZTR speed limit of the GA method. Percentages of FLT are highlighted which compare the theoretical profiles (Fig. 1) with the GA at the speed boundary in terms of the percentage increase in copper losses. The Cu loss increase from zero speed to the limit is minimal and highlights the proposed methods ability to maintain optimally minimal rms current with increasing speed. Given this minimal increase over the 1000rpm ZTR speed range, a memory saving could use only two current waveforms, specifically the waveform corresponding to 600rpm used from zero to 600rpm and the 1000rpm current waveform for the remainder of the ZTR speed range. This reduced memory storage approach is applicable at all torque levels.

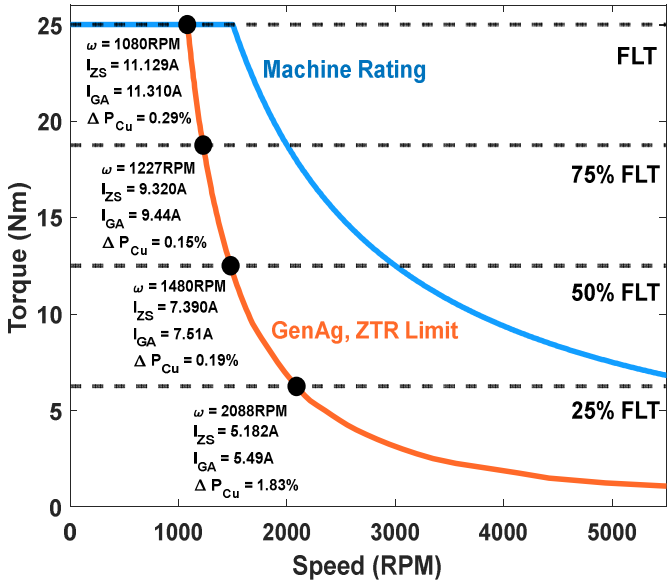

Fig.8 GA ZTR speed range and machine $T-\omega$ curve.

VI. Conclusion

This paper presented a Genetic Algorithm design for eliminating torque ripple and improving an SRMs efficiency, in a current profiling control scheme. The illustrated design produces profiles within the FLT speed range and inherently optimizes phase copper losses within the ZTR speed range. Simulations validated this and a comparison was made with current profiles produced by a commonly utilized GA generates ZTR currents that result in less than 1% increased Cu losses above the theoretical minimum, over a wide speed and torque range. The design also displays an ability to utilize SRM negative torque production regions to effectively lower rms current for the given demand. The theoretical minimum current with ZTR method offers a benchmark for assessing torque ripple reduction approaches.

VII. Acknowledgements

The presented research was support by the EPSRC grant EP/R029504/1, Quietening waveforms.

VIII. References

[1] C. Gan, J. Wu, Q. Sun, W. Kong, H. Li and Y. Hu, "A Review on Machine Topologies and Control Techniques for Low-Noise Switched Reluctance Motors in Electric Vehicle Applications," *in IEEE Access, vol. 6,* pp. 31430-31443, 2018.

[2] S. Li, S. Zhang, T. G. Habetler and R. G. Harley, "Modeling, Design Optimization, and Applications of Switched Reluctance Machines—A Review," *in IEEE Transactions on Industry Applications, vol. 55, no. 3,* pp. 2660-2681, May-June 2019.

[3] Z. Q. Zhu and D. Howe, "Electrical Machines and Drives for Electric, Hybrid, and Fuel Cell Vehicles," *in Proceedings of the IEEE, vol. 95, no. 4,* pp. 746-765, April 2007.

[4] Z. Yang, F. Shang, I. P. Brown and M. Krishnamurthy, "Comparative Study of Interior Permanent Magnet, Induction, and Switched Reluctance Motor Drives for EV and HEV Applications," *in IEEE Transactions on Transportation Electrification, vol. 1, no. 3,* pp. 245-254, Oct. 2015.

[5] D. -H. Lee, T. H. Pham and J. -W. Ahn, "Design and Operation Characteristics of Four-Two Pole High-Speed SRM for Torque Ripple Reduction," *in IEEE Transactions on Industrial Electronics, vol. 60, no. 9,* pp. 3637-3643, Sept. 2013.

[6] E. Bostanci, M. Moallem, A. Parsapour and B. Fahimi, "Opportunities and Challenges of Switched Reluctance Motor Drives for Electric Propulsion: A Comparative Study," *in IEEE Transactions on Transportation Electrification, vol. 3, no. 1,* pp. 58-75, March 2017.

[7] Cheok, and Y. Fukuda, ‘‘A new torque and flux control method for switched reluctance motor drives,’’ *IEEE Transactions on Power Electronics, vol. 17, no. 4,* pp. 543-557, Jul. 2002.

[8] R. B. Inderka and R. W. A. A. De Doncker, "DITC-direct instantaneous torque control of switched reluctance drives," *in IEEE Transactions on Industry Applications, vol. 39, no. 4,* pp. 1046-1051, July. 2003.

[9] M. V. de Paula and T. A. d. S. Barros, "A Sliding Mode DITC Cruise Control for SRM With Steepest Descent Minimum Torque Ripple Point Tracking," *in IEEE Transactions on Industrial Electronics, vol. 69, no. 1,* pp. 151-159, Jan. 2022.

[10] Q. Sun, J. Wu and C. Gan, "Optimized Direct Instantaneous Torque Control for SRMs With Efficiency Improvement," *in IEEE Transactions on Industrial Electronics, vol. 68, no. 3,* pp. 2072-2082, March 2021.

[11] C. Mademlis and I. Kioskeridis, "Performance optimization in switched reluctance motor drives with online commutation angle control," *in IEEE Transactions on Energy Conversion, vol. 18, no. 3,* pp. 448-457, Sept. 2003.

[12] D. S. Schramm, B. W. Williams and T. C. Green, "Torque ripple reduction of switched reluctance motors by phase current optimal profiling," PESC '92 Record. *23rd Annual IEEE Power Electronics Specialists Conference,* June-July. 1992.

[13] J. Ye, B. Bilgin and A. Emadi, "An Extended-Speed Low-Ripple Torque Control of Switched Reluctance Motor Drives," *in IEEE Transactions on Power Electronics, vol. 30, no. 3,* pp. 1457-1470, March 2015.

[14] F. Al-Amyal, L. Al Quraan and L. Szamel, "Torque Sharing Function *Optimization for Extended Speed Range Control in Switched* Reluctance Motor Drive," *2020 IEEE 3rd International Conference and Workshop in Óbuda on Electrical and Power Engineering (CANDO-EPE), 2020,* pp. 119-124.

[15] R. Abraham and S. Ashok, "Data-Driven Optimization of Torque Distribution Function for Torque Ripple Minimization of Switched Reluctance Motor," *2020 International Conference for Emerging Technology (INCET), 2020,* pp. 1-6.

[16] L. Feng, X. Sun, X. Tian and K. Diao, "Direct Torque Control With Variable Flux for an SRM Based on Hybrid Optimization Algorithm," *in IEEE Transactions on Power Electronics, vol. 37, no. 6,* pp. 6688-6697, June 2022.

[17] B. Anvari, H. A. Toliyat and B. Fahimi, "Simultaneous Optimization of Geometry and Firing Angles for In-Wheel Switched Reluctance Motor Drive," *in IEEE Transactions on Transportation Electrification, vol. 4, no. 1, pp. 322-329, March 2018*